Influence of the Tropical Cyclones on Tropospheric Ozone: Possible Implication

Siddarth Shankar Das[1], M. Venkat Ratnam[2], K. N. Uma[1], K. V. Subrahmanyam[1], I.A.Girach[1], A. K. Patra[2],S. Aneesh[1], K.V. Suneeth[1], K. K. Kumar[1], A.P.Kesarkar[2], S.Sijikumar[1]and G. Ramkumar[1]*

[1]Space Physics Laboratory, Vikram Sarabhai Space Centre, Trivandrum-695022, India
[2]National Atmospheric Research Laboratory, Gadanki-517112, India

***e-mail : dassiddhu@yahoo.com**

Abstract. The present study examines the role of tropical cyclones in the enhancement of tropospheric ozone**.** The most significant and new observation reported is the increase in the upper tropospheric (10-16 km) ozone by 20-50 ppbv, which has extended down to the middle (6-10 km) and lower troposphere (< 6 km). The descent rate of enhanced ozone layer during the passage of tropical cyclone is 0.8-1 km/day, which is three times that of a clear-sky day (non-convective). Enhancement of surface ozone concentration by ~ 10 ppbv in day-time and 10-15 ppbv in the night-time is observed during a cyclone. Potential vorticity, vertical velocity and potential temperature obtained from numerical simulation, reproduces the key feature of the observations. A simulation study indicates the downward transport of stratospheric air into the troposphere. Space-borne observations of relative humidity indicate the presence of sporadic dry air in the upper and middle troposphere over the cyclonic region. These observations constitute quantitatively an experimental evidence of redistribution of stratospheric ozone during cyclonic storms.

[**Key words:** Stratosphere-troposphere exchange processes, tropopause, ozone, water vapour]

1. Introduction

Stratospheric ozone (O_3) layer found around 25-30 km altitude regulates the amount of ultraviolet radiation coming from the Sun to the Earth's surface. Ozone is an important greenhouse gas, which acts as an oxidant in the troposphere and has an important role in the climate forcing (*Forster et al*., 2007; *Pan et al*., 2015). One of the major consequences of the tropospheric ozone enhancement is on the living organisms, as it acts as a toxic agent among the air pollutants (*National Research Council*, 1991). Increase in the tropospheric ozone is considered to be due to (1) in-situ photochemical formation associated with lightning, advection, anthropogenic activities (e.g., *Jacobson,* 2002 and references therein), and (2) stratospheric flux (*Wild*, 2007 and reference therein; *Skerlak et al*., 2014). The tropopause, which acts a barrier between the troposphere and the stratosphere, plays a key role in controlling the flow of minor constituents from one layer to other. The increase of the ozone downward flux from the stratosphere to the troposphere not only increases the tropospheric ozone, but also decreases the stratospheric ozone. The ozone presence in the troposphere (intruded from the stratosphere) will further react with tropospheric water vapour and the tropospheric ozone gets destroyed. In principle, the total columnar ozone decreases and thus there will be an enhancement in the penetration of UV radiation to the Earth's surface.

In general, stratospheric air intrusion into the troposphere is observed over the middle and higher latitudes, which are linked with synoptic scale disturbances (e.g. *Stohl et al*., 2003). This downward flow is attributed to the dissipation of extra-tropical planetary and gravity waves in the stratosphere (*Holton et al*., 1995). *Stohl et al.* (2003), and *Bourqui and Trepanier* (2010) have reported the continuous downward flows from the stratosphere to the troposphere in much small time-scale over extra-tropics. In the global ozone budget, 25-50 % of tropospheric ozone source is from middle latitude stratospheric intrusion (*Bourqui and Trepanier*, 2010). *Appenseller and Davies* (1992) have also discussed that exchange between

56 the stratosphere and the troposphere (both directions) is highly episodic. There is much
57 observational evidence supporting the slow intrusion of stratospheric air into the troposphere
58 during cut-off lows (*Vaughan and Price*, 1989), high/low-pressure systems (*Davies and*
59 *Schuepbach*, 1994), the tropopause folds (*Sprenger and Wernli*, 2003) and in a rapid episodic
60 manner which generally triggered by overshooting convection, like a tropical cyclones
61 (*Loring et al.,* 1996*; Baray et al.,* 1999; *Cairo et al.,* 2008; *Das*, 2009; *Das et al.,* 2011; *Zhan*
62 *and Wang*, 2012; *Jiang et al*., 2015; *Venkat Ratnam et al*., 2016).The overshooting
63 convection associated with tropical cyclone can weaken the tropopause stability which plays
64 a key role in the stratosphere-troposphere exchange. In addition, turbulence caused due to
65 wind shear (*Shapiro,* 1976) and breaking of gravity wave (*Langford et al*., 1996) can also be
66 the causative mechanisms for the occurrence of stratospheric intrusion. A recent study by *Pan*
67 *et al.* (2015) has shown the enhancement of tropospheric ozone associated with the
68 thunderstorm event. Subsidence of stratospheric air is generally observed in the vicinity of
69 cyclone (*Appenzeller and Davies*, 1992; *Baray et al*., 1999; *Cairo et al., 2008; Leclair De*
70 *Bellevue et al.,* 2006, 2007*; Das*, 2009; *Das et al.,* 2011; *Venkat Ratnam et al*., 2016). Slow
71 stratospheric intrusion is reasonably well understood and is a regular phenomenon, whereas
72 the rapid intrusion needs to be understood in detail.

73 The increase in surface ozone is also linked with stratospheric intrusion (e.g. *Bourqui*
74 *and Trepanier,* 2010). Earlier studies have also shown the stratospheric air intrusion into the
75 troposphere is associated with the deep convection by tropopause perturbation using aircraft
76 measurement (*Dickerson et al*., 1987; *Poulida et al.,* 1996; *Stenchikov et al*., 1996; *Pan et al.*,
77 2015). *Stohl et al*. (2000) have shown that episodic stratospheric intrusion is associated with
78 severe weather condition which enhanced the surface ozone concentration.

79 The bands of the tropical cyclone have intense vertical extended cumulus cloud up to
80 UTLS region. These bands of the cloud are accompanied with updrafts, whereas downdrafts

81 are encounter between these bands. The eyewall region is characterised by local maximum
82 equivalent potential temperature, whereas minimum is found in the middle to upper
83 troposphere. The eyewall and radius of maximum winds increase with height. The low-
84 pressure core extended to UTLS region and the horizontal pressure gradient decreases with
85 height (*Koteswaram*, 1967). *Mitra* (1996) and *Das* (2009) reported the weakening of the
86 tropopause during the passage of tropical cyclone. Detail study on the dynamical and
87 thermodynamical structure of tropical cyclone can be found in *Hence and Houze* (2012) and
88 the review article on clouds in the tropical cyclone can be found in *Houze* (2010). Thus, the
89 tropical cyclones have an influence on stratosphere-troposphere exchange process which
90 causes air mass and energy transports in the troposphere and redistribution of stratospheric
91 ozone (e.g. *Jiang et al*., 2015). A complete review on the effect of the tropical cyclones on
92 the upper troposphere and lower stratosphere can be found in *Cairo et al*. (2008). In spite of
93 many observational and modelling studies, the exchange of air mass from the stratosphere to
94 the lower troposphere in short-time scale associated with tropical cyclones is still unclear and
95 further studies are needed. The present study addresses the influence of the tropical cyclones
96 quantitatively on the enhancement of tropospheric ozone by the stratospheric intrusion.

97 **2. Campaign details and the data analysis**

98 An intense campaign, named as 'Troposphere-Stratosphere Exchange-Cyclone (TSE-C)'
99 under the Climate And Weather of Sun-Earth System (CAWSES)-India phase-II programme
100 (*Pallamraju et al*., 2014) was conducted during two cyclone events. Under this campaign, a
101 series of ozonesondes were launched from Trivandrum (8.5^{o}N, 76.5^{o}E) during the intense
102 period of cyclonic storm Nilam from 30 October to 7 November 2012 and a very-severe
103 cyclonic storm Phailin from 11 to 15 October 2013.The ozonesondes used are EN-SCI (USA)
104 make, which were integrated with the GPS based radiosondes of i-Met make. These standard
105 ozonesonde are made up of the Electrochemical Concentration Cell (ECC) (*Komhyr et al*.,

106 1995). The uncertainty in the ozone measurements is 5-10 %. Table 1 also provides the
107 details of ozonesonde measurements conducted during the passage of these cyclonic storms.
108 Ozonesonde data was obtained at a fixed height resolution by down sampling at 100 m height
109 resolution by the linear interpolation method. The India Meteorological Department (IMD)
110 also launches ozonesonde launches every fortnight. The background profiles (non-convective
111 day at least for 3 days) is constructed by averaging the ozonesonde data (23 profiles) obtained
112 from the IMD combined with our observations from 1995-2013 for the month October over
113 Trivandrum. The IMD-ozonesonde used Brewer bubbler electrochemical sonde developed in
114 the Ozone Research Laboratory of the IMD. These IMD ozone sonde were compared with
115 ECC sondes and found that it is underestimated by 5-10 % in the troposphere (*Kerr et al*.,
116 1994; *Deshler et al.,* 2008), which is about <2 ppbv of the observed mean value. Detail
117 system description of IMD-Ozonesonde can be found elsewhere (*Sreedharan*, 1968;
118 *Alexander and Chatterjee,* 1980). There is no ozonesonde launch by IMD in this campaign.
119 The measurements of near-surface ozone are carried out using the online UV photometric
120 ozone analyser (Model AC32M) of Environment S.A, France. This ozone analyser works on
121 the principle of UV absorption of ozone at the wavelength 253.7 nm. The instrument has a
122 lower detection limit of 1 ppbv and 1% linearity. The data is sampled at an interval of 5
123 minutes.

124 The SAPHIR (Sondeur Atmospherique du Profild' Humidite Intertropical par
125 Radiometrie) on-board Megha-Tropiques satellite is a multichannel passive microwave
126 humidity sounder, measuring brightness temperatures in six channels located close to the
127 183.31GHz water vapor absorption line (±0.15, ±1.20, ±2.80, ±4.30, ±6.60 and ±11.0,GHz).
128 These channels allow retrieving the integrated relative humidity respectively between the
129 levels of 1000–850 hPa, 850–700 hPa, 700–550 hPa, 550–400 hPa, 400–250 hPa, and 250–
130 100 hPa. The radiometer has a cross-track scan of ±43°, providing a swath of 1705 km and a

10 km resolution at nadir. This data is also used for the qualitative analysis of the stratospheric air. The detail instrumentation can be found in *Raju* (2013), and retrieval algorithm and validation can be found in *Gohil et al*. (2012); *Mathur et al.* (2013) and *Venkat Ratnam et al*. (2013); *Subrahmanyam and Kumar* (2013), respectively.

Apart from the ozonesonde observations, a high-resolution numerical simulation using the Advanced Research Weather Research and Forecast (WRF-ARW) model version 3.6 has also been carried out for both the cases of the cyclones. The model domain has been configured with two nested domains of 60 km and 20 km horizontal resolution, and covers an area extending from 1^{o}S to 25^{o}N and 60^{o}E to 100^{o}E. The innermost domain has been used for the present study. The initial and lateral boundary conditions have been taken from ERA-Interim reanalysis on 0.75^{o} x 0.75^{o} continuously at every 6 hours. The present simulation was carried out with the model Physics options :(i) New Simplified Arakawa-Schubert (NSAS) (*Han and Pan*, 2011), (ii) Yonsei University (YSU) boundary layer scheme (*Hong et al*., 2006), (iii) Rapid Radiative Transfer Model (RRTM) long-wave radiation scheme (*Mlawer et al*., 1997), (iv) WRF Single Moment (WSM) 5 class microphysical scheme (*Hong et al*., 2004), and (v) NOAA land-surface scheme (*Smirnova et al*., 2000).

3. Meteorological background

The present experiments were conducted during the passage of the (1) cyclonic storm '**N**ilam**'** from 28 October to 1 November 2012 and (2) very severe cyclonic storm 'Phailin**'** from 4-14 October 2013 over the Bay of Bengal (BOB). The track of each tropical cyclones and outgoing long wave radiation (OLR) images (date and time are stamped) are shown in Figures 1a and 1b, respectively. The detailed bulletin can be found in www.imd.gov.in. During these campaigns, several ozonesondes were launched from Trivandrum, whenever the intensity of cyclones is maximum and the path/eye was close to the launching site. The details of each of the tropical cyclone used for present analysis are as follows:

3.1 Case-1 (Nilam)

A depression formed over the southeast of BOB (~9.5^{0}N, 86.0^{0}E) at 11:30 IST (IST=UT+5.5h) of 28 October 2012. It moved westwards and intensified into a deep-depression on the morning of 29 October 2012 over southwest BOB, about ~550 km south-southeast of Chennai. It continued to move westwards and intensified into a Cyclonic Storm, 'Nilam' in the morning of 30 October 2012 over southwest BOB. Then it moved north-northwest, crossed the north Tamilnadu coast near Mahabalipuram (12.6^{0}N, 80.2^{0}E), south of Chennai in the evening hours of 31October 2012. After the landfall the cyclonic storm, Nilam moved west-northwest and weakened gradually into a deep depression and then into a depression in the morning hours of 1 November 2012.

3.2 Case-2 (Phailin)

A low-pressure system was formed over Tenasserim coast (~12.^{0}N, 96^{0}E), on the early morning of 6 October 2013. It intensified into a depression over the same region on 8 October and then moved towards the west-north-westwards. It further intensified into a deep depression on the early morning of 9 October 2013 and then into a cyclonic storm, 'Phailin' in the evening hours. Moving north-westwards, it finally converted into a severe cyclonic storm in the morning hours of 10 October 2013 over east central BOB. The very severe cyclonic storm continued to move north-westwards and crossed Andhra Pradesh and Orissa coast near Gopalpur (19.2^{0}N, 84.9^{0}E) in the late evening of 12 October 2013. It further continued to move north-north-westwards after the landfall for some time and then northward and finally north-north-eastwards up to southwest Bihar. The system weakened gradually into a cyclonic storm from 13 October 2013 and finally the intensity decreased to a low-pressure system on 14 October 2013.

4. Results and Discussion

Figure 2 (a-b) shows the profiles of ozone mixing ratio (OMR) and relative humidity (RH) from ozonesonde measurements during the passage of the tropical cyclones Nilam (top panels) and Phailin (bottom panels). The background ozone profile is obtained by averaging individual profile (23 profiles) over Trivandrum of October from 1995-2013 and is shown by dotted lines in Figure 2. During the passage of Nilam on 30 October 2012, enhancement in tropospheric ozone (marked by horizontal arrows) from the background by 40-50 ppbv was observed in the height region between 8-9 km (~1 km width) and 11-14 km (~3 km width). These enhancements persisted till 31 October 2012 but at the height region reduced 6-7 km with a reduced width. However, the enhancement of about ~40 ppbv was still observed on 2 November 2012 but the height region decreased to 5-6 km. After two days, we had again observations from 5-7 November 2012. The height of enhanced ozone layer in the troposphere reduced to ~4 km (40 ppbv), ~3 km (30 ppbv) and ~1.5 km (20 ppbv) on 5, 6 and 7 November 2012, respectively. The present observation reveals that the downward propagation of the enhanced upper tropospheric ozone layer into the lower troposphere occurring in an episodic manner. The descent rate of the ozone rich layer from the upper troposphere to the boundary layer during Nilam is approximately estimated to be ~875 m/day. It is also noted that the corresponding RH profiles during Nilam did not decrease with increasing ozone mixing ratio except on 2 November 2012. A significant sudden decrease in RH is observed on 2 November 2012 at ~6 km, where the maximum enhancement (~ 70 ppbv) of the tropospheric ozone layer is observed. This indicates the presence of accumulated dry air at 6 km. As the stratospheric air is dry and ozone rich and thus there may be a possibility that on 2 November 2012 the accumulated dry ozone rich air at 6 km may be of stratospheric origin.

A similar phenomenon is also observed during the passage of Phailin. Intrusion from ~14 km to 6 km (marked by horizontal arrows) is clearly observed in the ozone profiles from 11-

15 October 2013. During Phailin, tropospheric ozone increases by 20-30 ppbv and the width of the enhanced ozone layer is larger than that observed during the Nilam. During Phailin, the descent rate of enhanced ozone layer from the upper troposphere to the boundary layer is estimated to be ~1000 m/day. The descent rate in the tropical non-convective region, under the assumption of no vertical winds, may be inferred from the radiative heating rate in the tropical clear-sky regions. *Gettelman et al*. (2004) estimated tropical clear-sky radiative heating rates by using ozone and water vapour sounding data together with the radiative transfer models and found -1 to -2 K/day in the troposphere. If the temperature lapse rate is 6-10 K/km in the upper troposphere, the descent rate is estimated to be 0.1-0.3 km/day. In the present observations, 0.8-1 km/day descent rate is estimated during the passage of tropical cyclones which is three times that of clear-sky (non-convective) days radiative subsidence. This may indicate that downward flow in association with the tropical cyclones (in their outer regions) enhanced the transport of the ozone from the stratosphere to the lower troposphere.

As discussed in the introductory section, significant perturbation in the tropopause due to deep convection will lead to the transport of ozone-rich stratospheric air into the troposphere. Figure 3 shows variation in the cold point tropopause height (CPT-H) and cold point tropopause temperature (CPT-T) derived from radiosonde measurements during (a) Nilam and (b) Phailin over Trivandrum. Significant perturbation in the tropopause height and the temperature are observed for both the cyclone cases. The climatological mean tropopause height and temperature over southern India (peninsular) are observed to be ~16.5 km and ~ 191 K (*Sunilkumar et al*., 2013). The CPT-H gradually decreased from 17.8 km on 30 October to 16.7 km on 2 November 2012 for Nilam. Afterwards, the CPT-H gradually increased and reached to 17. 5 km. Similarly for Phailin, the CPT-H decreases from 16.5 km on 11 October 2013 to 15.8 km on 12 October 2013 and then gradually increases. The height

229 above the tropopause (i.e. stratosphere) is in radiative equilibrium, whereas the height below
230 the tropopause (i.e. troposphere) is in radiative-convective equilibrium.

231 In addition to the profiling of ozone, we have the surface measurement of ozone and
232 solar flux during the Phailin. Figure 4 shows the time series of near-surface ozone mixing
233 ratio along with solar irradiation from 11 to 19 October 2013. As expected, clear diurnal
234 variability is observed in the time-series of surface ozone. In general, there are three main
235 mechanisms for the production of ozone in the atmospheric boundary layer: (1)
236 photochemical reaction via NOx and CO channel, (2) Bio-mass burning /fossils fuel, and (3)
237 lightning. However, *David and Nair* (2011) have shown the diurnal pattern of surface ozone
238 observed over Trivandrum is due to the mesoscale circulation, i.e., local sea and land breeze
239 and the availability of NOx. From 11 to 14 October the maximum and minimum average
240 peak of surface ozone are observed to be 24 and 1 ppbv, respectively, whereas from 14 to 18
241 October 2013, the maxima and minima are observed to be 35 and 10 ppbv, respectively. Even
242 though there was no solar radiation in the evening hours, there are enhancements in surface
243 ozone concentration (indicated by vertical arrows) on 14-15, 16-17, 18-19 October 2013. The
244 upper and lower average is indicated by horizontal solid and dash lines, respectively. The
245 ozone profiles obtained from ozonesonde measurements also show that enhanced ozone layer
246 propagates downward from the upper troposphere during 11-15 October 2013. There is a
247 possibility that the enhanced tropospheric ozone can further propagate downward to near-
248 surface in the presence of downdrafts. The enhancement in the surface ozone even after the
249 cut-off in solar radiation can be linked to the downward flow of upper tropospheric ozone in
250 the presence of downdrafts. Time-series of solar irradiation shows that there was not much
251 change in the radiation among the days 11-13 and 14-17 October 2013.This indicates that the
252 observed enhancement in the surface ozone is not due to change in the sunshine. Over the
253 observation site, land-breeze prevails during night-time. The change in night-time ozone

depends on the precursor gas (e.g. NO) concentration in land-breeze, which has a dependency on local precursor gas emission/human activity. Due to the cyclonic condition over Trivandrum, change in human activity during 11-17 October 2013 would not have happened considerably and Bio-mass burning may not be possible due to associated rains. The day-to-day variability of surface ozone over Trivandrum is ~ 9.5 ppbv (1-sigma standard deviation). The observed enhancement in surface ozone is found to be ~10 ppbv in the day-time and 10-15 ppbv in the night time. In a recent study by *Jiang et al.* (2015), an increase of surface ozone by 21-42 ppbv and surface nocturnal surface ozone levels exceeding 70 ppbv is observed in the region Xiamen and Quanzhou over the south-eastern coast of China before the Typhoon Hagibis landing. However, there are possible of an influence of lightening associated with cyclone and thus, other possibility of this surface ozone cannot be fully ruled out. A planned experiment by setting-up various ground-based instruments is required to rule out the enhancement of surface ozone.

Further, to support the present observations of stratospheric intrusion into the troposphere and further to surface, a dynamical analysis is carried out using WRF-ARW simulations. *Das et al.* (2011) and *Pan et al*. (2015) have shown the ability of WRF simulations during the tropical cyclone. Figure 5 shows the height-time cross-section of (a) vertical velocity along with potential vorticity (magenta line) and potential temperature (black line) contours, and (b) relative humidity along with equivalent potential temperature (black line) and zonal wind (grey line) for Nilam (left panels) and Phailin (right panels) over Trivandrum using WRF simulations. Figure 5 (a) shows the presence of strong updrafts (red) and downdrafts (blue) marked with rectangle box in the UTLS regions. Enhanced potential vorticity of 0.5-1.5 PVU is also observed vertically down from the stratosphere to the troposphere overlapping the downdraft regions. The potential temperature contours indicate (Fig.5 (a)) the presence of reduced stability during 29-31 October 2012 (Nilam) and 9-11 October 2013 (Phailin).

279 Height-time cross-section of relative humidity shown in Figure 5 (b) indicates
280 presence of dry air from UTLS region to the 2-4 km. The equivalent potential temperature
281 contours in Figure 5 (b) indicate that from the surface to ~8 km it is highly unstable for
282 vertical motion and favourable condition for the convection to take place during 29-31
283 October 2012 (Nilam) and 9-11 October 2013 (Phailin). During the same periods, from 10
284 km to the tropopause level, the vertical motion is suppressed and the atmosphere is found to
285 be statically stable to the un-staturated atmosphere. The present condition indicates the
286 presence of statically stable stratospheric air in the upper and middle troposphere. In addition,
287 strong wind shear is also observed in the UTLS region.
288 Similarly, Figure 6 shows the height-latitude cross-section of (a) vertical velocity along
289 with potential vorticity (magenta line) and potential temperature (black line) contours, and (b)
290 relative humidity cross-section along with equivalent potential temperature (black line) and
291 zonal wind (grey line) at 79^{o}E at 18 GMT on 30 October 2012 for Nilam (left panels) and 18
292 GMT on 10 October 2013 for Phailin (right panels) using WRF simulations. The vertical
293 velocity profiles shows the presence of downdraft (blue) followed by updraft (red) between
294 8-17^{o}N in the UTLS region in both the cyclone cases. Enhanced potential vorticity of 0.5-1.5
295 PVU is also observed vertically down from the stratosphere to the lower troposphere,
296 overlapping the downdraft regions. High potential vorticity in the troposphere is also a
297 signature of stratospheric air in the troposphere. It is true that enhanced potential
298 vorticity can also be due to diabatic processes associated with condensational heating but the
299 enhancement is only observed with the presence of downdraft in the UTLS region. The
300 potential temperature contours indicate the presence of reduced stability of the atmosphere at
301 this location and noticed that stable stratospheric air penetrated downward at 12-14^{o}N for
302 Nilam and 16-18^{o}N for Phailin. Relative humidity profiles indicate the presence of dry air at
303 ~ 8^{o}N which is in the vicinity of ozonesonde observational site. The equivalent potential

304 temperature contours in Figure 6 (b) indicate that from the surface to 10 km it is highly
305 unstable for vertical motion and favourable condition for the convection to take place at 6-
306 12^{o}N for Nilam and 12-18^{o}N for Phailin. In the same latitude regions from 10 km to the
307 tropopause level, the vertical motion is suppressed and the atmosphere is found to be
308 statically stable to the un-staturated atmosphere for both Nilam and Phailin. The present
309 condition indicates the presence of statically stable stratospheric air in the upper and middle
310 troposphere in the latitudinal cross-section at 79^{o}E at 18 GMT on 30 October 2012 and 10
311 October 2013. Numerical simulation reproduced the key features supports the possibility of
312 stratospheric air intrusion into the troposphere during the passage of tropical cyclone.
313 To get further insight, relative humidity derived from SAPHIR on-board the Megha-
314 Tropiques satellite is used. The relative humidity (daily mean) shown is an average over 12-
315 14 passes per day. Figure 7 shows the height-time intensity plot of daily mean relative
316 humidity during the passage of the cyclones: Nilam (left panel) and Phailin (right panel). The
317 grid is averaged from 4-8^{o}N and 83-88^{o}E. Strong dry air intrusion originated in the lower
318 stratosphere is observed between 23-27 October 2012 (Nilam) and 12-18 October 2013
319 (Phailin). In both the cyclones, dry air (low humidity region) reached down to the altitude of
320 8 km. For the perception of the spatial distribution of relative humidity, a latitude-longitude
321 plot of relative humidity averaged over different pressure level is shown in Figure 8. The low
322 value of relative humidity i.e., the presence of dry air on the same day of enhanced ozone
323 mixing ratio in between 5 and 10 km indicate the possibility of dry air present in the
324 troposphere is of stratospheric origin. The present observations provide strong evidence for
325 the influence of the tropical cyclone on the air mass exchange from the stratosphere to the
326 lower troposphere and redistribution of stratospheric ozone. Further trajectory and chemical
327 analysis are required to verify this and to quantify the amount of mass exchange taking place
328 between the stratosphere and the troposphere.

5. Summary and Conclusions

Important results brought out in the present analysis during the passage of a cyclonic storms Nilam (2012) and Phailin (2013) are summarized below:

a) Increase in the upper tropospheric ozone by 20-50 ppbv from its climatological mean is observed.

b) The upper tropospheric ozone propagates downwards to the lower troposphere at a rate of 0.8-1 km/day.

c) About 10 ppbv in the day-time and 10-15 ppbv in the night-time increase in the surface ozone is noticed

d) Significant variation in the cold-point tropopause altitude and temperature associated with tropical cyclone as that of the climatological mean are noticed.

In the present study, the descent of stratospheric air into the troposphere has been deduced indirectly from a combination of ozone and meteorological observations, and modelling. The study clearly reveals that the cyclones play a vital role in changing the atmospheric composition apart from general weather phenomena.

Acknowledgments

Results reported in this manuscript are from the experimental campaign, TSE-C, conducted under the CAWSES-India Phase-II program, which is fully funded by the Indian Space Research Organisation (ISRO), Government of India and authors sincerely acknowledge the same. The authors would like to thank all the technical and scientific staff of the Space Physics Laboratory (SPL) who participated in this STE-C campaign. The India Meteorological Department (IMD) is highly acknowledged for providing the climatological ozonesonde data. K.V. Suneeth and S. Aneesh are thankful to ISRO for providing doctoral fellowship during the study period. Authors would like to thank the editor and all the three

354 reviewers for their constructive comments and suggestions which helped in the improvement
355 of the manuscript.
356
357

358 **References**

359 Appenzeller, C. and Davies, H.C.: 1992. Structure of stratospheric intrusions into the
360 troposphere. Nature, 358, 570 – 572, doi:10.1038/358570a0.

361 Alexander G., and Chatterjee K.: 1980. Atmospheric ozone measurements in India. Proc.
362 Indian Natn. Sci. Aca., 46, A, 234-244.

363 Baray, J.L., Ancellet, G., Randriambelo, T., Baldy, S., 1999.: Tropical cyclone Marlene and
364 stratosphere-troposphere exchange. J. Geophys. Res.,104, 13953– 13970, doi :
365 10.1029/1999JD900028.

366 Bourqui, M. S., and Trepanier P. Y., 2010.:, Descent of deep stratospheric intrusions during
367 the IONS August 2006 campaign. J. Geophys. Res., 115, D18301,
368 doi:10.1029/2009JD013183.

369 Cairo, F., Buontempo, C., MacKenzie, A.R., Schiller, C., Volk, C.M., Adriani, A., Mitev, V.,
370 Matthey, R., Di Donfrancesco, G., Oulanovsky, A., Ravegnani, F., Yushkov, V., Snels,
371 M., Cagnazzo, C., Stefanutti, L., 2008.: Morphology of the tropopause layer and lower
372 stratosphere above a tropical cyclone : a case study on cyclone Davina (1999). Atmos.
373 Chem. and Phy. 8, 3411-3426, doi:10.5194/acp-8-3411-2008.

374 Das, S.S., 2009.: A new perspective on MST radar observations of stratospheric intrusions
375 into troposphere associated with tropical cyclone. Geophys. Res. Lett, 36, L15821, doi :
376 10.1029/2009GL039184.

377 Das, S.S., Sijikumar, S., Uma, K.N., 2011.: Further investigation on stratospheric air
378 intrusion into the troposphere during the episode of tropical cyclone: Numerical
379 simulation and MST radar observations. Atmos. Res., 101, 928-937,
380 doi:10.1016/j.atmosres.2011.05.023.

Davies, T.D. and Schuepbach, E., 1994.: Episodes of high ozone concentration at the earth's surface resulting from transport down from the upper troposphere-lower stratosphere : a review and case studies. Atmos. Env., 28, 53-68, doi:10.1016/1352-2310(94)90022-1.

David, L. M., and Nair, P.R. 2011.: Diurnal and seasonal variability of surface ozone and NOx at a tropical coastal site: Association with mesoscale and synoptic meteorological conditions.116, D10303, doi : 10.1029/2010JD015076.

Deshler, T., et al., 2008.: Atmospheric comparison of electrochemical cell ozonesondes from different manufacturers, and with different cathode solution strengths: The Balloon Experiment on Standards for Ozonesondes. J. Geophys. Res., 113, D04307, doi:10.1029/2007JD008975.

Dickerson, R. R., et al. 1987.: Thunderstorms: An important mechanism in the transport of air pollutants, Science. 235, 460–465, doi : 10.1126/science.235.4787.460.

Forster, P.M., Bodeker, G., Schofield, R., Solomon, S., Thompson, D., 2007.: Effect of ozone cooling in the tropical lower stratosphere and upper troposphere. Geophys. Res. Lett, 34, L23813, doi : 10.1029/2007GL031994.

Gettelman, A., Forster, P. M. de F., Fujiwara, M., Fu, Q., Vömel, H., Gohar, L. K., Johanson, C., and Ammerman, M., 2004.: Radiation balance of the tropical tropopause layer. Journal of Geophysical Research, 109, D07103, doi: 10.1029/2003JD004190.

Gohil, B.S., Gairola, R.M., Mathur, A.K., Varma, A.K., Mahesh, C., Gangwar, R.K., Pal, P.K., 2012.: Algorithms for retrieving geophysical parameters from the MADRAS and SAPHIR sensors of the Megha-Tropiques satellite: Indian scenario. Q. J. Royal Meteo. Soc., 139, 954-963, doi : 10.1002/qj.2041.

Han, J. and Pan, H.L., 2011.: Revision of convection and vertical diffusion schemes in the NCEP global forecast system. Weather Fore. 26, 520–533, doi:10.1175/WAF-D-10-05038.1.

406 Hence, D.A., and Houze Jr. R.A., 2012.: Vertical Structure of Tropical Cyclone Rainbands as
407 Seen by the TRMM Precipitation Radar. 69, 2644-2661, doi : 10.1175/JAS-D-11-
408 0323.1.
409 Holton, J.R., Haynes, P.T., and Mclntyre, M.E., 1995.: Stratosphere-troposphere exchange.
410 Review Geophys., 33, 403 – 439, doi : 10.1029/95RG02097.
411 Hong, S.Y., Dudhia, J., and Chen, S.H., 2004.: A revised approach to ice microphysical
412 processes for the bulk parameterization of cloud sand precipitation. Mon. Weather
413 Rev., 132, 103–120, doi : 10.1175/1520-0493(2004)132<0103:ARATIM>2.0.CO;2.
414 Hong, S.Y., Noh, Y., and Dudhia, J., 2006.: A new vertical diffusion package with an
415 explicit treatment of entrainment processes. Mon. Wea. Rev., 134, 2318–2341, doi :
416 10.1175/MWR3199.1.
417 Houze Jr. R., 2010.: Review Clouds in Tropical Cyclones. Mon. Weather Rev., 138, 293-344,
418 doi : 10.1175/2009MWR2989.1.
419 Jacobson, M.Z., 2002.: Control of fossil-fuel particulate black carbon and organic matter,
420 possibly the most effective method of slowing global warming. J. Geophys. Res.,
421 107(D19), 16-22, doi : 10.1029/2001JD001376.
422 Jiang, Y. C., Zhao, T. L., Liu, J., Xu, X. D., Tan, C. H., Cheng, X. H., Bi, X. Y., Gan, J. B.,
423 You, J. F., and Zhao, S. Z., 2015: Why does surface ozone peak before a typhoon
424 landing in southeast China?. Atmos. Chem. Phys., 15, 13331-13338, doi:10.5194/acp-
425 15-13331-2015.
426 Kerr, J. B., Fast , H., McElroy, C.T., Oltmans, S.J., Lathrop, J.A., Kyro, E., Paukkunen, A.,
427 Claude, H., Köhler, U., Sreedharan, C.R., Takao, T., and Tsukagoshi, Y.,1994.: The
428 1991 WMO International Ozonesonde Intercomparison at Vanscoy. Canada, Atmos.
429 Ocean, 32, 685–716, doi : 10.1080/07055900.1994.9649518.

Komhyr, W.D., Barnes, R.A., Brothers, G. B., Lathrop, J.A., and Opperman, D.P.,1995.: Electrochemical concentration cell ozonesonde performance evaluation during STOIC 1989. J. Geophys. Res., 100, 9231-9244, doi : 10.1029/94JD02175.

Koteswaram, P., 1967.: On the structure of hurricanes in the upper troposphere and lower stratosphere. Mon. Weather Rev., 95, 541-564, doi : 10.1175/1520-0493(1967)095<0541:OTSOHI>2.3.CO;2.

Langford, A. O., Masters, C. D., Proffitt, M. H., Hsie, E.-Y., and Tuck, A. F., 1996.: Ozone measurements in a tropopause fold associated with a cut-off low system. Geophys. Res. Lett., 23, 2501–2504, doi :10.1029/96GL02227.

Leclair, De Bellevue J., R´echou, A., Baray, J.L., Ancellet, G., and Diab, R..D., 2006.: Signatures of stratosphere to troposphere transport near deep convective events in the southern subtropics. J. Geophys. Res., 111, D24107, doi:10.1029/2005JD006947.

Leclair, De Bellevue J., Baray, J. L., Baldy, S., Ancellet, G., Diab, R.D., and Ravetta, F., 2007.: Simulations of stratospheric to tropospheric transport during the tropical cyclone Marlene event. Atmos. Env., 41, 6510–6526, doi:10.1016/j.atmosenv.2007.04.040.

Loring Jr, R.O., Fuelberg, H.E., Fishman, J., Watson, M.V., and Browell, E.V., 1996.: Influence of a middle-latitude cyclone on tropospheric ozone distributions during a period TRACE A. J. Geophys. Res., 101, D19, 23941-23956, doi : 10.1029/95JD03573.

Mathur, A. K., Gangwar, R.K., Gohil, B.S., Deb, S.K., Kumar, P., Shukla, M.V., Simon, B., and Pal, P.K., 2013.: Humidity profile retrieval from SAPHIR on-board the Megha-Tropiques. Current Sci., 104, 1650-1655.

Mitra, A. P., 1996.: Troposphere-stratosphere coupling and exchange at low latitude. Adv. Space Phys., 17, 1189-1197, doi:10.1016/0273-1177(95)00735-W.

Mlawer, E, J., Taubman, S.J., Brown, P.D., Iacono, M.J., and Clough, S.A., 1997.: Radiative transfer for inhomogeneous atmosphere: RRTM, a validated correlated-k model for the long wave. J. Geophys. Res., 102 (D14), 16663–16682, doi : 10.1029/97JD00237.

National Research Council (1991), Rethinking the Ozone Problem in Urban and Regional Air Pollution. 1051 Committee on Tropospheric ozone formation and measurement, Natl. Acad. Press, Washington, D.C.

Pallamraju, D., Gurubaran, S., and Venkat Ratnam, M., 2014.: A brief overview on the special issue on CAWSES-India Phase II program. J. Atmos. Sol.-Terr. Phys., 121, 141-144, doi : 10.1016/j.jastp.2014.10.013.

Pan, L.L. et al., 2015.: Thunderstorms enhance tropospheric ozone by wrapping and shedding stratospheric air, Geophy. Res. Lett., 41, 7785-7790, doi : 10.1002/2014gl061921.

Poulida, O., Dickerson, R. R., and Heymsfield, A., 1996.: Stratosphere troposphere exchange in a midlatitude mesoscale convective complex. J. Geophys. Res., 101, 6823–6836, doi:10.1029/95JD03523.

Raju, G., 2013. Engineering challenges in the Megha-Tropiques. Current Sci., 104, 1662-1670.

Shapiro, M. A., 1976.: The role of turbulent heat flux in the generation of potential vorticity in the vicinity of upper-level jet stream systems. Mon. Weather Rev., 104, 892–906, doi :10.1175/1520-0493(1976)104<0892:TROTHF>2.0.CO;2.

Škerlak, B., Sprenger, M., and Wernli, H., 2014: A global climatology of stratosphere–troposphere exchange using the ERA-Interim data set from 1979 to 2011. Atmos. Chem. Phys., 14, 913-937, doi:10.5194/acp-14-913-2014, 2014.

Smirnova, T.G., Brown, J.M., Benjamin, S.G., and Kim, D., 2000.: Parameterization of cold season processes in the MAPS land-surface scheme. J. Geophys. Res., 105 (D3), 4077–4086, doi : 10.1029/1999JD901047.

478 Sprenger, M. and Wernli, H., 2003.: A northern hemispheric climatology of cross-tropopause
479 exchange for the ERA15 time period (1979–1993). J. Geophys. Res., 108(D12), 8521,
480 doi:10.1029/2002JD002636.
481 Sreedharan, C. R., 1968.: An Indian electrochemical Ozonesonde. J. Phys. E. Sci. Inst-Sr.,
482 2(1), 995-997.
483 Stenchikov, G., Dickerson, R., Pickering, K., Ellis Jr., W., Doddridge, B., Kondragunta, S.,
484 Poulida, O., Scala, J., and Tao, W.-K., 1996.: Stratosphere-troposphere exchange in a
485 midlatitude mesoscale convective complex: 2. Numerical simulations. J. Geophys.
486 Res., 101, 6837–6851, doi:10.1029/95JD02468.
487 Stohl, A., Wernli, H., Bourqui, M., Forster, C., James, P., Liniger, M. A., Seibert, P., and
488 Sprenger, M., 2003.: A new perspective of stratosphere-troposphere exchange. Bull.
489 Am. Met. Soc. 84, 1565-1573.70, doi: 10.1175/BAMS-84-11-1565.
490 Stohl, A., and et al., 2000.: The influence of stratospheric intrusions on alpine ozone
491 concentrations. Atmos. Environ., 34, 1323–1354, doi:10.1016/S1352-2310(99)00320-
492 9.
493 Subrahmanyam, K.V. and Kumar, K.K., 2013.: Megha-Tropiques/SAPHIR measurements of
494 humidity profiles: validation with AIR Sand global radiosonde network. Atmos. Meas.
495 Tech.-Disc., 6, 11405–11437, doi:10.5194/amtd-6-11405-2013.
496 Sunilkumar, S.V.,Babu, A., and Parameswaran, K., 2013.: Mean structure of the tropical
497 tropopause and its variability over the Indian longitude sector. Clim. Dyn. 40, 1125-
498 1140. doi : 10.1007/s00382-012-1496-8.
499 Vaughan, G. and Price, J., 1989.: Ozone transport into the troposphere in a cut-off low event,
500 Ozone in the atmosphere (ed. R.Bojkov& P. Fabian). 415-418,A. Deepak Publishing
501 Hampton (USA).

Venkat Ratnam, M., Basha,,G., Murthy, B.V.K., and Jayaraman, A., 2013.: Relative humidity distribution from SAPHIR experiment on board Megha-Tropiques satellite mission: Comparison with global radiosonde and other satellite and reanalysis data sets. J. Geophys. Res., 118, 9622–9630, doi : 10.1002/jgrd.50699.

Venkat Ratnam, M., Ravindra Babu, S., Das, S.S., Basha, G., Krishnamurthy, B.V., and Venkateswararao, B., 2016.: Effect of tropical cyclones on the Stratosphere-Troposphere Exchange observed using satellite observations over north Indian Ocean. Atmos. Chem. Phys. Discuss., doi:10.5194/acp-2015-988.

Wild, O., 2007.: Modelling the global tropospheric ozone budget: Exploring the variability in current models. Atmos. Chem. Phys., 7(10), 2643–2660, doi:10.5194/acp-7-2643-2007.

Zhan, R. and Wang, Y., 2012.: Contribution of tropical cyclones to stratosphere-troposphere exchange over the northwest Pacific: Estimation based on AIRS satellite retrievals and ERA-Interim data. J. Atmos. Res., 117. D12112, doi:10.1029/2012JD017494.

Figure Captions

Figure 1. (a)Track of cyclones Nilam and Phailin (top panels) and (b) its Outgoing Long wave Radiation (OLR) wave radiation at 14:30 GMT on 30 Oct. 2012 (Nilam) and 9:00 GMT on 10 Oct. 2013 (Phailin). In each panel, date and time are mentioned along the track. In the first panel, 18-1/11 indicates 18 GMT of 1 November 2012 and similarly followed for others. The blue star in Fig.1(a) indicates the Ozonesonde launching site Trivandrum.

Figure 2. (a) Profiles of ozone mixing ratio (OMR) (dark black line) and relative humidity (grey line) for individual days during the passage of tropical cyclones (a) Nilam and (b) Phailin. The mean ozone mixing ratio profile for non-convective days (as control day) is shown in dotted line. The mean profile is obtained by averaging ozone data over Trivandrum for the month of October from 1995-2013. Horizontal arrows indicate the height of enhanced ozone.

Figure 3. Variation of cold point tropopause height (CPT-H) and cold point tropopause temperature (CPT-T) derived from temperature measurement by ozonesonde launched during the passage of tropical cyclones (a) Nilam and (b) Phailin over Trivandrum.

Figure 4. Time series of surface ozone mixing ratio (thick line) along with solar radiation (dotted line) from 00 IST on 11 October 2013 to 23:55 IST on 19 October 2013. Solid and dotted horizontal lines indicate the mean maximum and minimum surface ozone. The vertical arrows indicate the nocturnal enhancement of surface ozone. The data is collected with 5 minutes resolution.

Figure 5. Height-time cross-section of (a) vertical velocity along with potential vorticity (magenta line) and potential temperature (black line) contours, and (b) relative humidity along with equivalent potential temperature (black line) and zonal wind (grey line) for Nilam (left panels) over Trivandrum (8.5^{o}N,76.9^{o}E) from 27 October to 2 November 2012 and Phailin (right panels) from 7 to 12 October 2013. Rectangle boxes indicate the presence

of strong updrafts and downdrafts and the dry air between stratosphere and troposphere. The above parameters are obtained from WRF simulation.

Figure 6. Same as Figure 5 but at 79^{o}E at 18 GMT on 30 October 2012 for Nilam (left panels) and 18 GMT on 10 October 2013 for Phailin (right panels). **Figure 7.** Pressure-time cross-section of relative humidity obtained from SAPHIR onboard Megha-Tropiques satellite during the cyclones Nilam (left panel) from 15 October to 10 November 2012 and Phailin (right panel) from 2 to 22 October 2013. The data is averaged over from 4^{o}N to 8^{o}N and 83^{o}E to 88^{o}E.

Figure 8. Latitude-longitude distribution of relative humidity derived from SAPHIR onboard Megha-Tropiques at different pressure levels (stamped on each panel) for Nilam (25 October 2012) and Phailin (14 October 2013). The data is averaged for one day which is about 12-14 passes at different timings and arrows indicate the presence of dry air.

Table Caption

Table 1. Details of ozonesonde launched from Trivandrum including the historical data for control day analysis.

Figure 1. (a)Track of cyclones Nilam and Phailin (top panels) and (b) its Outgoing Long wave Radiation (OLR) wave radiation at 14:30 GMT on 30 Oct. 2012 (Nilam) and 9:00 GMT on 10 Oct. 2013 (Phailin). In each panel, date and time are mentioned along the track. In the first panel, 18-1/11 indicates 18 GMT of 1 November 2012 and similarly followed for others. The blue star in Fig.1(a) indicates the Ozonesonde launching site Trivandrum.

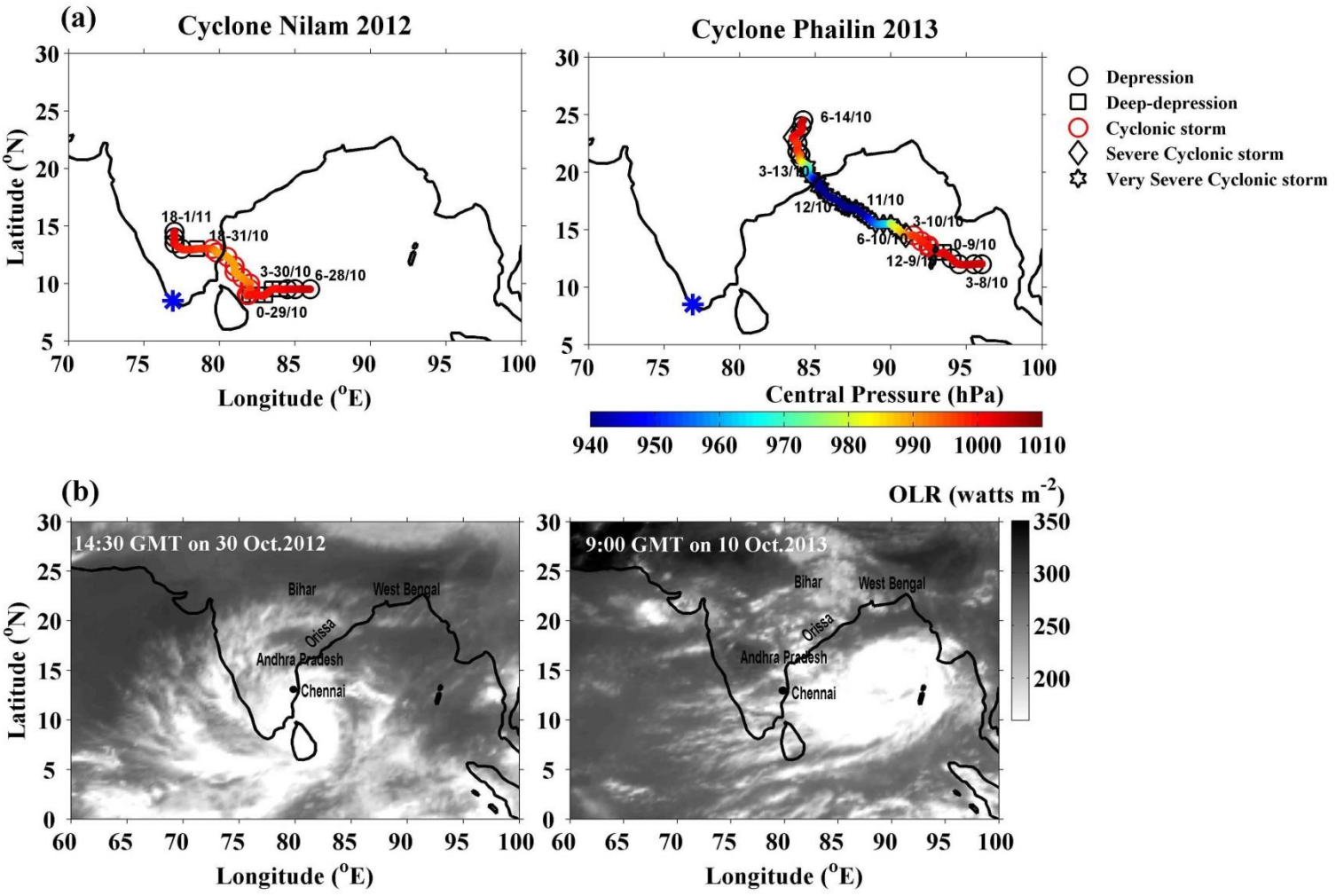

Figure 2. (a) Profiles of ozone mixing ratio (OMR) (dark black line) and relative humidity (grey line) for individual days during the passage of tropical cyclones (a) Nilam and (b) Phailin. The mean ozone mixing ratio profile for non-convective days (as control day) is shown in dotted line. The mean profile is obtained by averaging ozone data over Trivandrum for the month of October from 1995-2013. Horizontal arrows indicate the height of enhanced ozone.

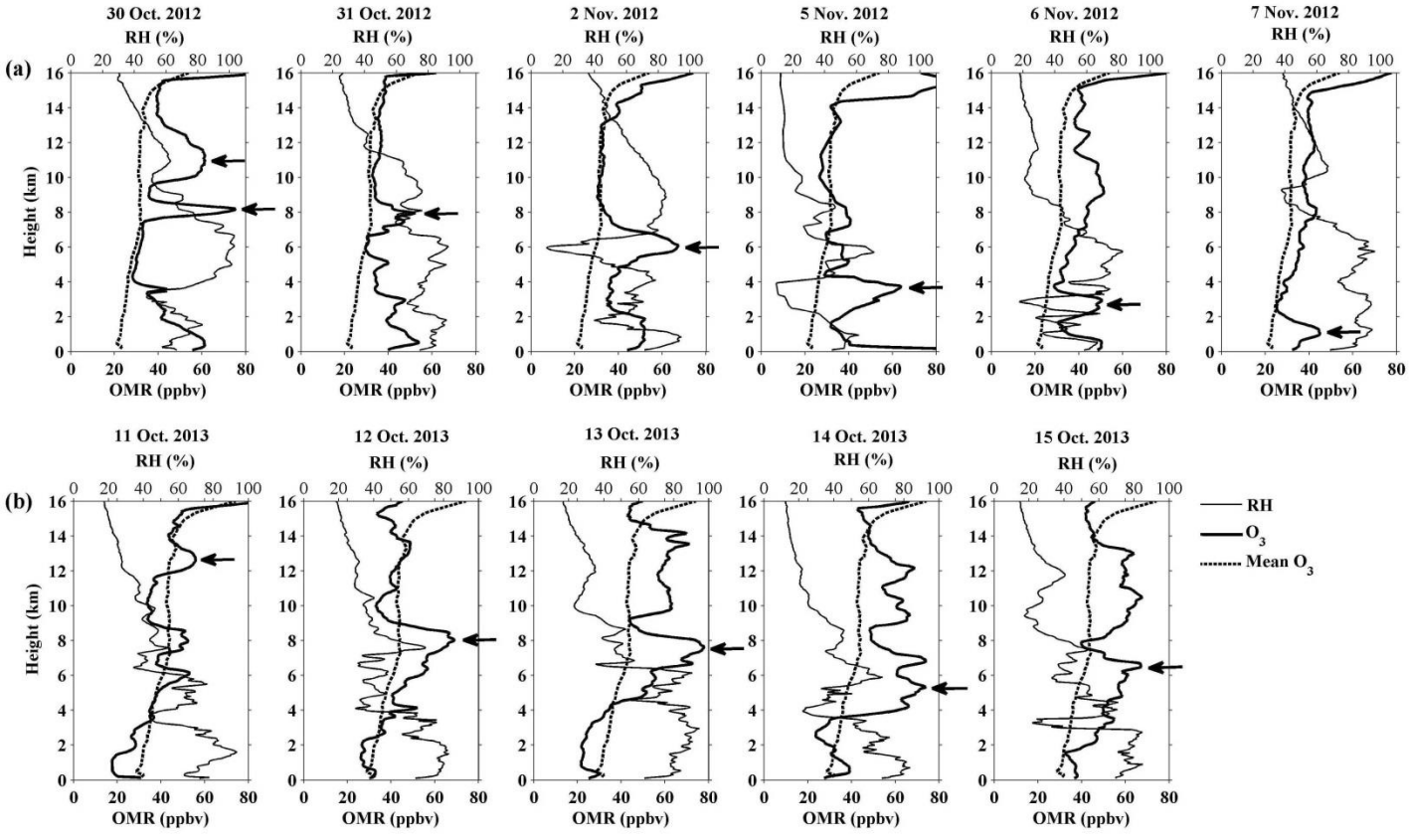

Figure 3. Variation of cold point tropopause height (CPT-H) and cold point tropopause temperature (CPT-T) derived from temperature measurement by ozonesonde launched during the passage of tropical cyclones (a) Nilam and (b) Phailin over Trivandrum.

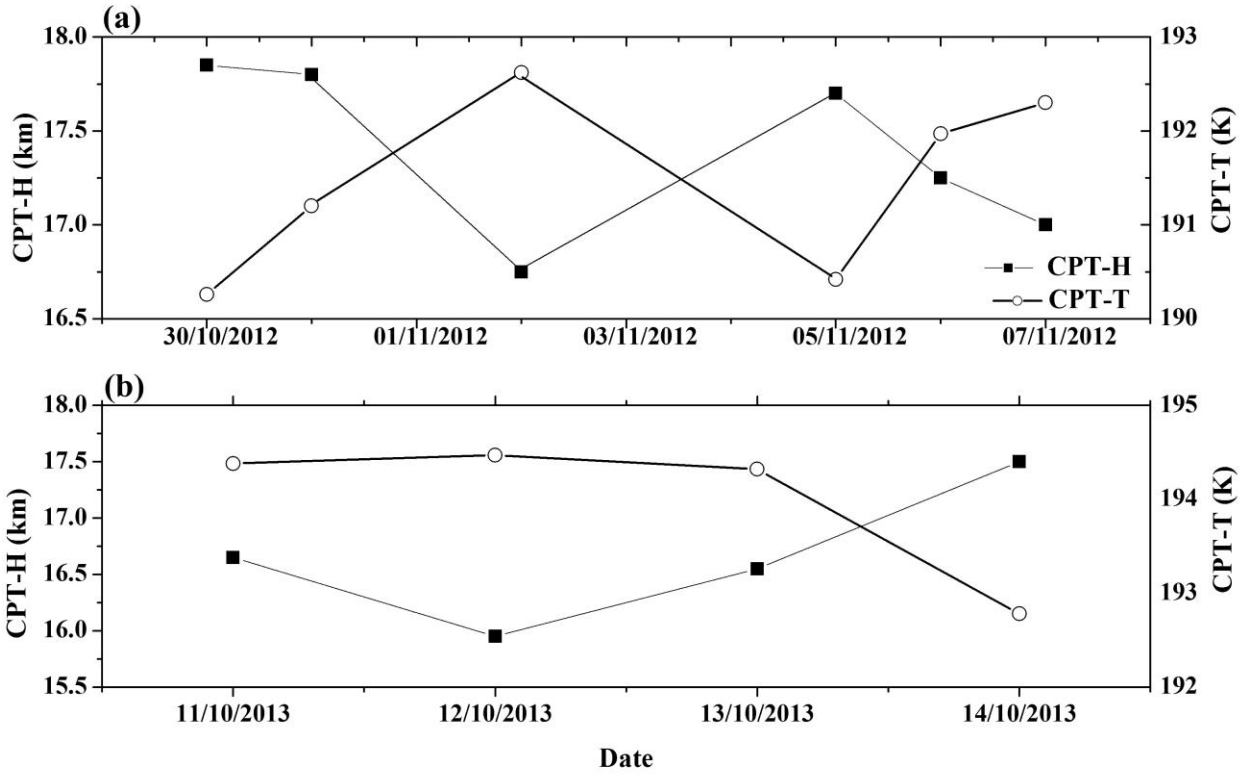

Figure 4. Time series of surface ozone mixing ratio along with solar radiation from 00 IST on 11 October 2013 to 23:55 IST on 19 October 2013. Solid and dotted horizontal lines indicate the mean maximum and minimum surface ozone. The vertical arrows indicate the nocturnal enhancement of surface ozone. The data is collected every 5 min.

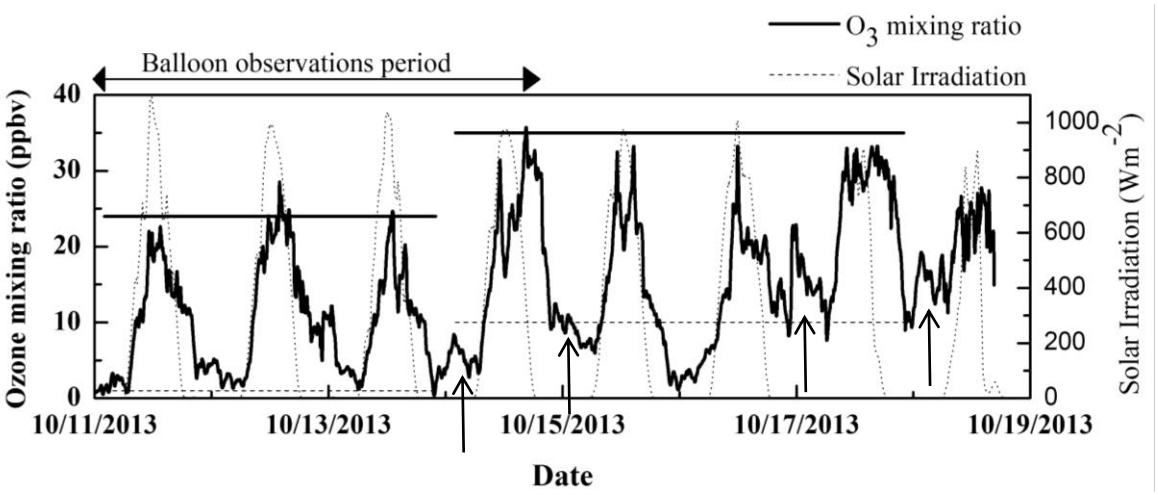

Figure 5. Height-time cross-section of **(a)** vertical velocity along with potential vorticity (magenta line) and potential temperature (black line) contours, and **(b)** relative humidity along with equivalent potential temperature (black line) and zonal wind (grey line) for Nilam (left panels) over Trivandrum (8.5°N,76.9°E) from 27 October to 2 November 2012 and Phailin (right panels) from 7 to 12 October 2013. Rectangle boxes indicate the presence of strong updrafts and downdrafts and the dry air between stratosphere and troposphere. The above parameters are obtained from WRF simulation.

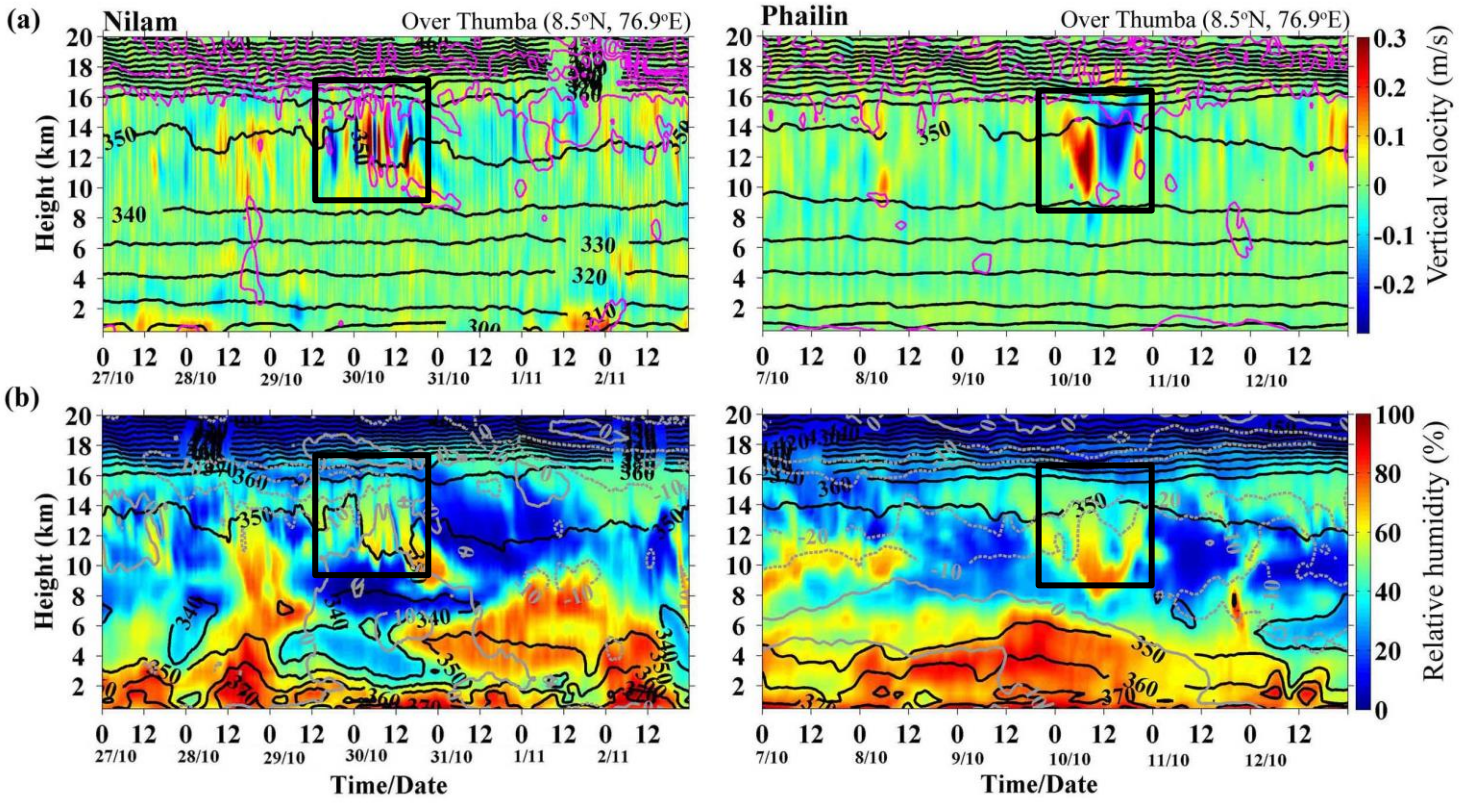

Figure 6. Height-latitude cross-section of **(a)** vertical velocity along with potential vorticity (magenta line) and potential temperature (black line) contours, and **(b)** relative humidity cross-section along with equivalent potential temperature (black line) and zonal wind (grey line) at 79^{o}E at 18 GMT on 30 October 2012 for Nilam (left panels) and 18 GMT on 10 October 2013 for Phailin (right panels). The above parameters are obtained from WRF simulation.

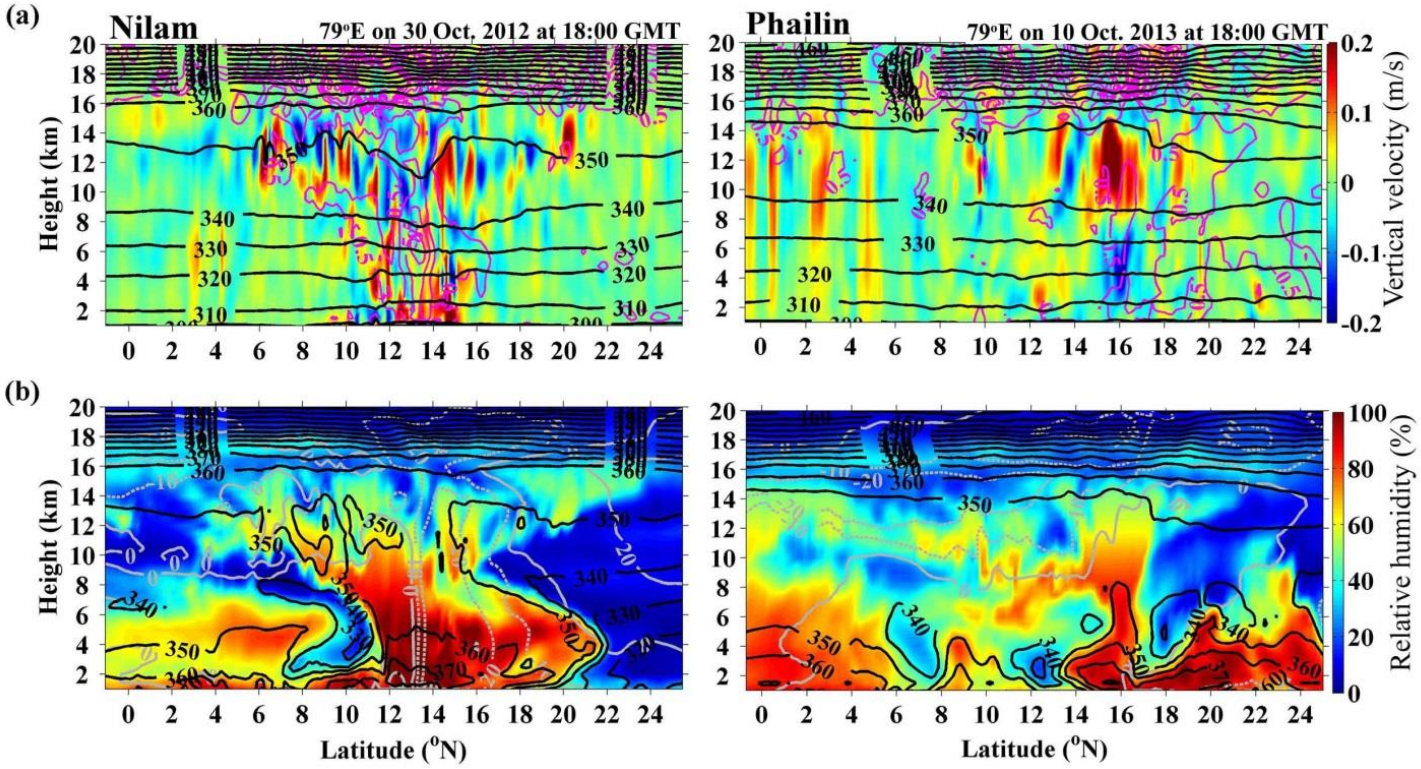

Figure 7. Pressure-time cross-section of relative humidity obtained from SAPHIR onboard Megha-Tropiques satellite during the cyclones Nilam (left panel) from 15 October to 10 November 2012 and Phailin (right panel) from 2 to 22 October 2013. The data is averaged over from 4°N to 8°N and 83°E to 88°E.

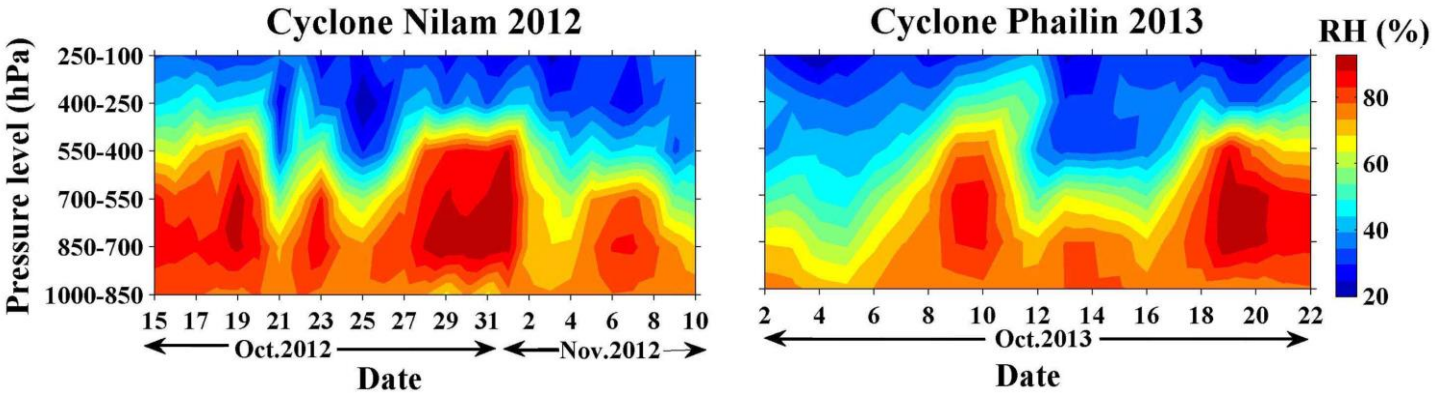

Figure 8. Latitude-longitude distribution of relative humidity derived from SAPHIR onboard Megha-Tropiques at different pressure levels (stamped on each panel) for Nilam (25 October 2012) and Phailin (14 October 2013). The data is averaged for one day which is about 12-14 passes at different timings and arrows indicate the presence of dry air.

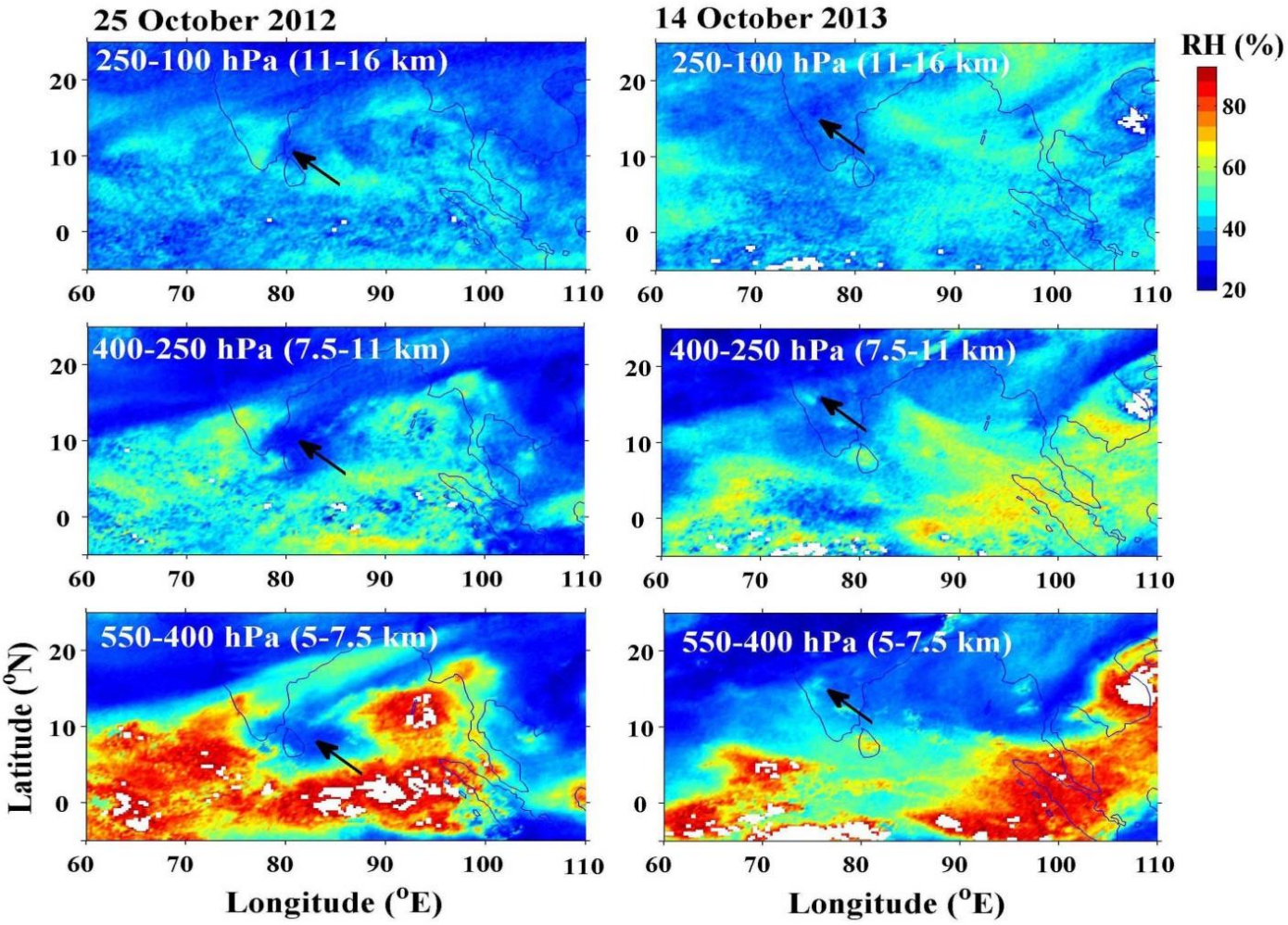

Table 1. Details of ozonesonde launched from Trivandrum including the historical data for control day analysis.

Description	Date
Cyclone Nilam	30 Oct. 2012
	31 Oct. 2012
	2 Nov. 2012
	5 Nov. 2012
	6 Nov. 2012
	7 Nov. 2012
Cyclone Phailin	11 Oct. 2013
	12 Oct. 2013
	13 Oct. 2013
	14 Oct. 2013
	15 Oct. 2013
Control Days	24 Oct. 1995
	25 Oct. 1995
	7 Oct. 1998
	21 Oct. 1998
	4 Oct. 2000
	4 Oct. 2002
	1 Oct. 2003
	15 Oct. 2003
	30 Oct. 2003
	27 Oct. 2004
	28 Sep. 2005
	25 Oct. 2006
	7 Oct. 2009
	12 Oct. 2011
	13 Oct. 2011
	14 Oct. 2011
	19 Oct. 2011
	27 Oct. 2011
	3 Oct. 2012
	14 Oct. 2012
	28 Oct. 2013
	29 Oct. 2013